RESEARCH PAPER

Root system size and root hair length are key phenes for nitrate acquisition and biomass production across natural variation in Arabidopsis

Jérôme De Pessemier[1,†,‡], Taraka Ramji Moturu[1,‡], Philippe Nacry[2], Rebecca Ebert[3], Hugues De Gernier[1,4,5], Pascal Tillard[2], Kamal Swarup[6], Darren M. Wells[6], Jim Haseloff[7], Seth C. Murray[8], Malcolm J. Bennett[6], Dirk Inzé[4,5], Christopher I. Vincent[3], and Christian Hermans[1,*]

[1] Crop Production and Biostimulation Laboratory, Interfacultary School of Bioengineers, Université libre de Bruxelles, B-1050 Brussels, Belgium
[2] Institute of Plant Science Montpellier, Université de Montpellier, CNRS, INRAE, Institut Agro, 34060 Montpellier, France
[3] Citrus Research and Education Center, Horticultural Sciences Department, Institute of Food and Agricultural Sciences, University of Florida, Lake Alfred, FL, USA
[4] Department of Plant Biotechnology and Bioinformatics, Ghent University, 9052 Ghent, Belgium
[5] VIB Center for Plant Systems Biology, 9052 Ghent, Belgium
[6] School of Biosciences, University of Nottingham, Sutton Bonington Campus, Loughborough LE12 5RD, UK
[7] Department of Plant Sciences, University of Cambridge, Cambridge CB2 3EA, UK
[8] Department of Soil and Crop Sciences, Texas A&M University, College Station, TX 77843, USA
[†] Present address: SESVANDERHAVE N.V., B-3300 Tienen, Belgium.

[‡] These authors contributed equally to this work.
* Correspondence: christian.hermans@ulb.be

Abstract

The role of root phenes in nitrogen (N) acquisition and biomass production was evaluated in 10 contrasting natural accessions of *Arabidopsis thaliana* L. Seedlings were grown on vertical agar plates with two different nitrate supplies. The low N treatment increased the root to shoot biomass ratio and promoted the proliferation of lateral roots and root hairs. The cost of a larger root system did not impact shoot biomass. Greater biomass production could be achieved through increased root length or through specific root hair characteristics. A greater number of root hairs may provide a low-resistance pathway under elevated N conditions, while root hair length may enhance root zone exploration under low N conditions. The variability of N uptake and the expression levels of genes encoding nitrate transporters were measured. A positive correlation was found between root system size and high-affinity nitrate uptake, emphasizing the benefits of an exploratory root organ in N acquisition. The expression levels of *NRT1.2/NPF4.6*, *NRT2.2*, and *NRT1.5/NPF7.3* negatively correlated with some root morphological traits. Such basic knowledge in Arabidopsis demonstrates the importance of root phenes to improve N acquisition and paves the way to design eudicot ideotypes.

Keywords: Arabidopsis, mineral nutrition, natural variation, nitrate uptake, root hairs, root morphology.

Introduction

The root is an important organ in achieving more sustainable global food production. Mineral nutrition of plants is central to reaching global food security for the rapidly growing world population (Spiertz, 2010; Fanzo *et al.*, 2020). More food is needed from the same land area, while reducing the environmental impact of agriculture (Pradhan *et al.*, 2015). To this end, there is a pressing need to develop new crop cultivars with better capture and use of soil resources. Root morphology, especially the dynamic three-dimensional exploration of the available soil volume, is critical in plant mineral nutrition and nutrient use efficiency (White, 2019).

Nitrogen (N) is quantitatively the most important nutrient required by crops. Mineral N fertilizer manufacturing comes with a huge energetic cost and releases large quantities of greenhouse gases. Yet over half of all applied fertilizer is currently lost, with additional detrimental consequences on the environment and human health (Martinez-Dalmau *et al.*, 2021). Agronomic N use efficiency (NUE) is calculated as crop biomass per unit of N fertilizer applied. The uptake (NUpE) and utilization (NUtE) efficiencies are two NUE components (Moll *et al.*, 1982). NUpE reflects the ability of the plant to take up the N available in soil, and NUtE represents the transfer of N taken up to harvestable products. One sensible target to enhance NUpE is manipulating root morphology (Lynch and Brown, 2012; Li *et al.*, 2016). Root traits have been largely absent from crop breeding programs due to the difficulty in observing root morphology below ground (Louvieaux *et al.*, 2020a, b). A 'steep, cheap, and deep' root system could be a key target for developing genotypes with greater N capture (Lynch, 2013, 2019; Li *et al.*, 2016; Pierret *et al.*, 2016). Nitrate is the predominant N form in most agricultural soils and acts a major determinant of root morphology (Kiba and Krapp, 2016). Local nitrate sources stimulate lateral root growth, whereas high nitrate concentrations throughout the growth medium have a systemic inhibitory effect on lateral root formation (Zhang *et al.*, 2007). *Arabidopsis thaliana* L. (Arabidopsis) has become universally recognized as a model for studying root morphogenesis with unprecedented depth of knowledge (Banda *et al.*, 2019; Vangheluwe and Beeckman, 2021). Knowledge of the role of nitrate signaling in the regulation of lateral root development in Arabidopsis has been gradually building (Sun *et al.*, 2017; Asim *et al.*, 2020; Vidal *et al.*, 2020).

In addition to overall root organ architecture and size, root hairs should be taken into account in crop improvement programs (Lynch, 2019) as they provide a low-resistance pathway for collecting mineral nutrients, disproportionately enhancing uptake of less mobile elements (Jungk, 2001). Root hair formation is also modulated by nitrate availability (Vatter *et al.*, 2015; Jia and von Wirén, 2020). Canales *et al.* (2017) found that some root hair-defective Arabidopsis mutants had reduced nitrate uptake compared with their wild types.

Although root hair density has been attributed to greater uptake of nitrate and other mineral nutrients, modeling of diffusion has long suggested that root hair distribution and length are the most important traits in enhancing mineral nutrient diffusion (Nye, 1966; Itoh and Barber, 1983; Keyes *et al.*, 2013). Despite longstanding interest in the impact of root hairs in water and nutrient uptake, only a few studies have addressed root hairs at the whole root organ level or have compared the impacts of various root hair phenotypes (e.g. density, length, or total root hair production) on plant growth.

The uptake of nitrate from the soil solution occurs at the plasma membrane of root cells through the action of well-characterized transport systems. The low-affinity transport system (LATS) is active at elevated nitrate concentrations (>0.5–1 mM) and the high-affinity transporter system (HATS) at low (<1 mM) concentrations. Both systems include inducible and constitutive carriers (reviewed in Vidal *et al.*, 2020; Muratore *et al.*, 2021). In Arabidopsis, the NITRATE TRANSPORTER1/PEPTIDE TRANSPORTER FAMILY (NPF, formerly NRT1/PTR) (Léran *et al.*, 2014) and the NITRATE RELATED TRANSPORTER 2 (NRT2) families play a role in nitrate uptake at the root level (Orsel *et al.*, 2002). At low substrate concentrations, NRT2.1 and NRT2.2 are responsible for three-quarters and one-fifth, respectively, of the HAT activity (Li *et al.*, 2010). At high substrate levels, NRT1.1/NPF6.3 and NRT1.2/NPF4.6 have a major but non-exclusive contribution to the total LATS activity, indicating the existence of other low-affinity systems (Huang *et al.*, 1999; Krouk *et al.*, 2006). Additional transporters such as NRT1.4/NPF6.2, NRT1.5/NPF7.3, NRT1.7/NPF2.13, NRT1.8/NPF7.2, or NRT2.4, 5 play roles in root to shoot allocation and remobilization from source to sink (Chiu *et al.*, 2004; Lin *et al.*, 2008; Fan *et al.*, 2009; Li *et al.*, 2010; Kiba *et al.*, 2012; Lezhneva *et al.*, 2014; Drechsler *et al.*, 2015; Meng *et al.*, 2016; Li *et al.*, 2017a). Furthermore, NRT1.1 also has a signaling function (Krouk *et al.*, 2010) and plays a role in lateral root proliferation in response to local nitrate sources (Remans *et al.*, 2006a; Mounier *et al.*, 2014; Maghiaoui *et al.*, 2020), and high root branching in nutrient-rich zones may be a desirable phenotype to enhance NUE. Additionally, there are several examples in crops of nitrate transporter expression manipulation increasing plant growth, source to sink remobilization, and NUE (Hu *et al.*, 2015, Fan *et al.*, 2016; Chen *et al.*, 2020).

Natural populations of Arabidopsis, which grow in a wide range of soil conditions, provide a rich and diverse genetic resource to study N-related adaptive differences in root morphology (De Pessemier *et al.*, 2013) and NUE processes (North *et al.*, 2009; Chardon *et al.*, 2010; Masclaux-Daubresse and Chardon, 2011). Through the exploration of natural variation, several genes and alleles regulating root morphological traits in response to N were uncovered (Gifford *et al.*, 2013; Jia *et al.*, 2019, 2020, 2021; Rosas *et al.*, 2013). Furthermore,

key NUE–related traits identified in the model species could be applicable to economically important crop species (Li *et al.*, 2017b; Stephenson *et al.*, 2019).

This study examined the relationships between root characteristics, nitrate uptake capacity, and biomass production. A core set of 10 Arabidopsis accessions with contrasting root morphologies was assembled on the basis of a larger preliminary screen. First, a comparative analysis with two divergent nitrate supplies was conducted for biomass production, root morphology, root hair characteristics, root growth dynamics, nitrate uptake rate, and expression levels of genes encoding nitrate transporters. Second, the relationships between these variables were evaluated. Root characteristics which could be an asset for improving N capture and biomass production are discussed.

Materials and methods

Plant material and growth conditions

The following *A. thaliana* accessions were obtained from the Nottingham Arabidopsis Stock Centre or INRAE Versailles Genomic Resource Center: Borky-1 (Bor-1), C24, Cape Verde Islands-0 (Cvi-0), Columbia-0 (Col-0), Le Pyla-1 (Pyl-1), Llagostera-0 (Ll-0), Noordwijk-1 (Nok-1), Oystese-0 (Oy-0), Petergof, and Tsushima-0 (Tsu-0). The two T-DNA insertion lines of *NRT1.5/NPF7.3* (SALK_043036 and SALK_063393) in the Col-0 background were obtained from Q. Ma, College of Pastoral Agriculture Science and Technology, Lanzhou University, Lanzhou, PR China. Prior to performing the experiments, seed stocks were regenerated in the same environment. Seed surfaces were sterilized with 70% (v/v) ethanol for 10 min and in 20% (v/v) HClO for 5 min. They were sown on 1× Murashige and Skoog medium modified with nitrate as the only source of N (Hermans *et al.*, 2010), 1% (w/v) sucrose and pH adjusted to 5.7. Each square Petri plate (12 × 12 cm) contained 50 ml of medium solidified with 0.8% (w/v) agar (Plant agar, Duschefa Biochemie). Seeds were stratified for 2 d at 4 °C in the dark then vertically incubated in a culture chamber at a temperature of 20 °C and a daylight regime of 16 h light (45 μmol photons m^{-2} s^{-1})/8 h darkness. Six days after germination on a medium containing 10 mM KNO_3 (N+), seedlings were transferred for an additional 6 d to an identical medium or one with 0.01 mM KNO_3 (N−). Potassium chloride (9.99 mM) was added to prevent K depletion in the N− medium. The mutant lines were grown uninterruptedly for 14 d on medium containing 0.1 mM KNO_3+9.9 mM KCl, 1 mM KNO_3+9 mM KCl, or 10 mM KNO_3. In total, four plates containing five seedlings per accession and per N condition were prepared. One Petri plate is shown in Supplementary Fig. S1. The root systems were scanned with an EPSON Scan Perfection V30, at a resolution of 400 dpi for root morphology analysis and 1700 dpi for root hair quantification. Eventually, the root and shoot were separated, and the pooled organs of five plants were weighed.

Time-based root image acquisition

The growth dynamics of the primary root and of the first emerged lateral root were monitored with an automated system for image acquisition (Wells *et al.*, 2012). For robot imaging, seeds were plated following the procedure as described above. Seedlings grew at a temperature of 23 °C and daylight regime of 12 h light (150 μmol photons m^{-2} s^{-1})/12 h darkness. Upon transfer to N+ or N− media, seedlings were placed in the controlled environment housing the measuring equipment. Plates were imaged every 30 min for 120 h. The system used a belt-driven linear actuator to position two cameras with a capacity of 20 plates. A near-infrared light source allowed roots to be imaged in darkness.

Quantitative analysis of the root morphology

Root morphological traits (Table 1) were quantified from low-resolution scanner and automated system images using RootNav software, and trait measurement computations were then performed with the RootNav Viewer (Pound *et al.*, 2013).

Root hair quantification

Root hairs were quantified using high-resolution scanner images according to Vincent *et al.* (2016). Briefly, the method required root hairs of small samples to be manually traced. Using the manual tracing, a logistic model was fit to predict which image pixels showed or did not show root hairs. This model was then applied to all root hair areas in the image, from which root hair traits (Table 1) were calculated.

15N tracer assays

The HATS/LATS-mediated nitrate influxes were determined by ^{15}N labeling. The protocol of root influx by short-term ^{15}N labelling is commonly used to characterize the nitrate uptake rate of Arabidopsis accessions cultivated *in vitro* (Remans *et al.*, 2006b; Laugier *et al.*, 2012; Ota *et al.*, 2020). Briefly, seedlings grown with 0.01 mM or 10 mM KNO_3 were carefully detached from the agar surface. Dispersed roots were sequentially bathed in a round Petri dish (5 cm diameter) filled with (i) 10 ml of 0.1 mM $CaSO_4$ solution for 1 min; (ii) 10 ml of N-free basal liquid medium supplemented with 0.1 mM (HATS) or 10 mM (LATS)

Table 1. Abbreviations of the measured traits

Biomass production traits	
R	Root biomass
S	Shoot biomass
R+S	Total biomass
R:S	Root to shoot biomass ratio
Root morphological traits	
L_{PR}	Length of primary root
N_{LR}	Number of lateral roots >1 mm
ΣL_{LR}	Sum of lateral root lengths
D_{LR}	Density of lateral roots in the zone between the first and last lateral roots
SRL	Specific root length =$(L_{PR}+\Sigma L_{LR})$/R
$PRGR_{dark/light}$	Primary root growth rate measured in the dark/light period
$LRGR_{dark/light}$	Lateral root growth rate measured in the dark/light period
Root hairs traits	
A_{RH}	Total projected two-dimensional area of root hairs
ML_{RH}	Mean length of root hairs
RL_{RH}	Root hair-forming root length
^{15}N uptake studies	
^{15}N Q_R	^{15}N quantity in root
^{15}N Q_S	^{15}N quantity in shoot
^{15}N $Q_{R:S}$	Root to shoot ^{15}N amount
^{15}N HATS/LATS	^{15}N influx rate mediated by HATS or LATS per hour and per plant = $(^{15}N Q)_R+(^{15}N Q)_S$/5×60

K^{15}NO$_3$ (Sigma-Aldrich) for 5 min; and (iii) 10 ml of 0.1 mM CaSO$_4$ solution for 1 min. Roots were able to disperse in the different incubation solutions. They were separated from shoots immediately after the last transfer to CaSO$_4$ and placed in tin capsules (Santis Analytical). Plant organs were dried for 48 h at 70 °C, and dry biomass was weighed. The ^{15}N abundance in plant tissues was measured with an integrated system for continuous flow isotope ratio mass spectrometry (Euro-EA elementar Analyzer, EuroVector SPA; IRMS Isoprime, Elementar). The calculation of the instantaneous [^{15}N]HATS/LATS-mediated influx is included in Table 1.

RNA extraction and qPCR assays

Total RNA was extracted from whole root organs (Aurum Total RNA Mini Kit, Biorad, USA) and submitted to a second purification step (RNA Clean and Concentrator-5, Zymo Research). Reverse transcription was done with the GoScript Reverse cDNA Synthesis kit (Promega). The Janus Automated Workstation (PerkinElmer) handled all pipetting for PCRs in a final volume of 5 µl using LightCycler 480 SYBR Green I Master mix (Roche). Quantitative PCRs (qPCRs) were performed with the LightCycler 480 (Roche): pre-incubation at 95 °C for 10 min, 45 cycles of 95 °C for 30 s, 60 °C for 60 s followed by melting curves. Primers are listed in Supplementary Table S1. Levels of *ACTIN 2* (*ACT2*) and *UBIQUITIN 10* (*UBQ10*) were used as normalization factors.

Statistical treatment

ANOVA was performed using a linear model implemented with the lmer() command in the {lme4} package (Bates *et al.*, 2015) in R statistical language (R Core Team, 2019). The model consisted of fixed effects for accession (G), nitrate treatment (N), and their interactions (G×N) with individual plant observations nested within plate as the experimental unit. To estimate the variance components for each trait, the same model was fit as fully random using standard least squares (restricted maximum likelihood method) in JMP version 15.0 (SAS Institute Inc.). Best linear unbiased predictions (BLUPs) of G, N, and G×N interactions were estimated.

To determine relationships between phenotypic traits, a principal component analysis (PCA) was conducted with XLSTAT. To determine the effects of phenotypic traits on total biomass production, a linear regression model was fit using JMP and variance components were extracted.

Pearson correlations were calculated for all combinations of phenotypic traits at each N condition using R and XLSTAT (http://www.xlstat.com). Hierarchical classification of accessions was carried out using MatLab software according to Ward's method. The PCA was also performed using XLSTAT software.

Hierarchical clustering analysis of the accessions was done using the Average method in R with all measured traits.

Results

Accessions exhibit variation in root morphological traits and root growth rates in response to nitrate supply

Following previous phenotyping screens carried out by De Pessemier *et al.* (2013), Gifford *et al.* (2013), and Jia *et al.* (2020), a panel of 10 Arabidopsis accessions with contrasting root morphologies was assembled. In the first experiment, seedlings grew on agar medium supplemented with 10 mM nitrate (N+) or 0.01 mM nitrate (N−). The morphological variation of whole root systems is presented in Fig. 1 and details of root hairs in Supplementary Fig. S2. All measured traits listed in Table 1 are presented in Fig. 2, and statistical treatment is summarized in Supplementary Table S2. First, the global response to the N supply was evaluated for the diverse set of accessions. The overall trend showed no significant ($P>0.05$) impact, either on the root fresh biomass (R) or on the specific root length (SRL) under N− compared with N+ conditions. The shoot fresh biomass (S) (−61%), the total biomass (R+S) (−46%), and the length of the primary root (L$_{PR}$) (−6%) decreased significantly ($P<0.01$) in N− compared with N+ conditions. The root to shoot (R:S) biomass ratio (+151%), the number of lateral roots that visibly (>1 mm) emerged from the primary root (N$_{LR}$) (+39%), the sum of lateral root length (ΣL$_{LR}$) (+30%), the lateral root density (D$_{LR}$) (+48%), the total projected two-dimensional area (A$_{RH}$) (+85%), the mean length of root hairs (ML$_{RH}$) (+56%), and the root hair-forming root length (RL$_{RH}$) (+110%) increased significantly ($P<0.01$) in N− compared with N+ conditions.

The extent to which variations in biomass production, root morphology, and root hair traits (Fig. 2) were due to genetic differences between accessions (G), nitrate treatment differences (N), genetic differences in the level of response to nitrate treatment (G×N), and unexplained experimental errors (residuals) was assessed (Fig. 3; Supplementary Table S3). Most of the variation for root biomass (R) and root morphological traits (L$_{PR}$, N$_{LR}$, ΣL$_{LR}$, and D$_{LR}$) was due to G (in the range of 68–77%), while the variation for other biomass (S, R+S, R:S) and root hair (A$_{RH}$, ML$_{RH}$, RL$_{RH}$) traits was mainly attributable to N (in the range of 42–84%). The G×N interaction effect was negligible for most traits, except for A$_{RH}$ (17%) and ML$_{RH}$ (33%). Therefore, the root biomass or root morphological traits were largely unresponsive to N treatment under these culture conditions. In contrast, shoot biomass and RL$_{RH}$ showed large genotype-independent plasticity to N treatment. Only two root hair traits (A$_{RH}$ and ML$_{RH}$) showed moderate genotype-dependent plasticity to N treatment.

Next, the phenotypic variation between accessions was inspected (Fig. 2). The traits were significantly ($P<0.01$) different between accessions in both N treatments (Supplementary Table S2). The accessions Pyla-1 (Pyl-1) and Noordwijk-1 (Nok-1) produced low R biomass and very few N$_{LR}$ under both N treatments. In contrast, Borky-1 (Bor-1) and Petergof maintained important R biomass together with abundant and long lateral roots regardless of the N treatment. The accession C24 had the shortest L$_{PR}$ but elevated D$_{LR}$. Cape Verde Islands-0 (Cvi-0) produced the greatest S biomass and ML$_{RH}$ of all accessions in the N− condition (Supplementary Fig. S2). The reference Col-0 produced the lowest shoot biomass but had the greatest SRL in N− conditions. Other accessions, such as Llagostera-0 (Ll-0), Oystese-0 (Oy-0), and Tsushima-0 (Tsu-0) displayed characteristics similar to the average of the panel. We examined which accessions expressed noticeable G×N on
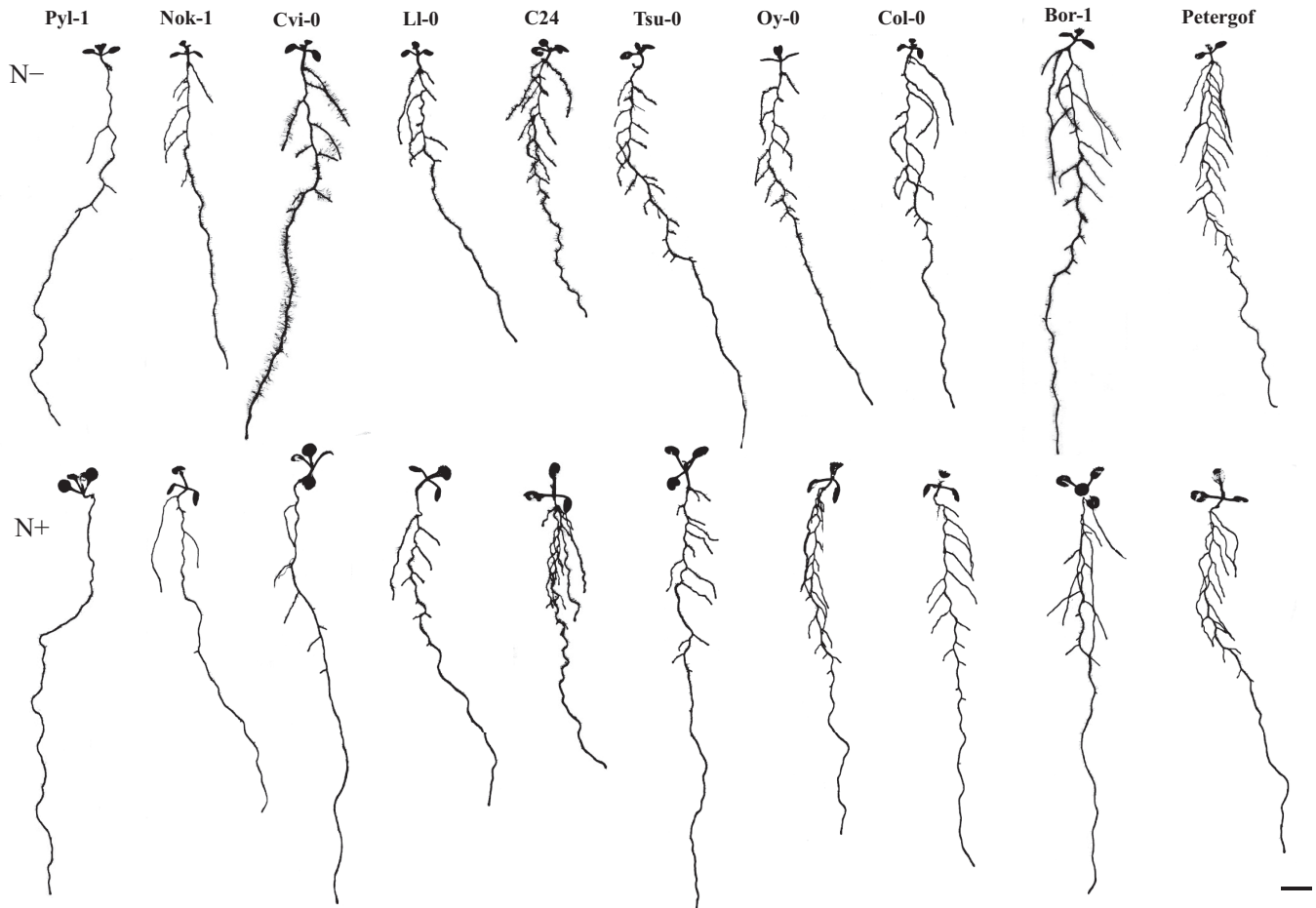
Fig. 1. Root phenotypes of Arabidopsis accessions in response to nitrate supply. Seedlings were germinated on a medium containing 10 mM nitrate (N+) and transferred 6 d after germination to a medium of the same concentration or 0.01 mM (N–). Pictures were taken 6 d after transfer. Scale bar: 1 cm.

root hair traits (Supplementary Table S3). The largest individual accession G×N observed was Cvi-0 for ML_{RH}. The Bor-1 and Pyl-1 accessions expressed noticeable G×N for A_{RH}. Pyl-1 also increased G×N for RL_{RH}. These G×N effects for root hair traits were unique, showing the major G×N across all of the traits in this study.

In the second experiment, the growth dynamics of the primary root and of the first emerged lateral root were monitored (Fig. 4). The primary root length increase was nearly constant from day to day, but the primary root growth rate (PRGR) fluctuated during 24 h. For most accessions, PRGR showed an abrupt decrease at the beginning of the light period, and a progressive increase during the dark period with a maximum at dawn (Fig. 4A, B). The average primary root growth rate was calculated during the light period ($PRGR_{light}$) and the dark period ($PRGR_{dark}$) over four monitoring cycles (Fig. 4C, D). The accession C24 had the slowest rates, with minimal variations between light and dark, while Tsu-0 had the fastest rates at both N concentrations. The growth rate of the first emerged lateral root followed the same oscillatory pattern, but

oscillations were much less synchronized than those of the primary root in most accessions (Fig. 4E, F).

Relationships between biomass production, root morphology, and root hair traits

Using the measures of the first and second experiments, a PCA captured the variation of biomass production, root morphology, root hairs, and root growth rate traits in response to the N treatment and between the accessions. The two first principal components (PC1 and PC2), respectively, explained 40.1% and 26.1% of the observed variance (Fig. 5A). The traits RL_{RH}, R:S, D_{LR}, A_{RH}, N_{LR}, and ΣL_{LR} (ranked by strength) showed the largest loadings on PC1, whereas R, $PRGR_{dark}$, L_{PR}, $PRGR_{light}$, and R+S had the greatest positive contribution to PC2. The traits A_{RH}, RL_{RH}, and ML_{RH} all had similar loadings in PC1 and PC2, suggesting possible covariance. The S biomass had equal loading on PC1 and PC2. With respect to the two first PCs, the N- and N+ treatments were easily distinguished, and groups of accessions with common features
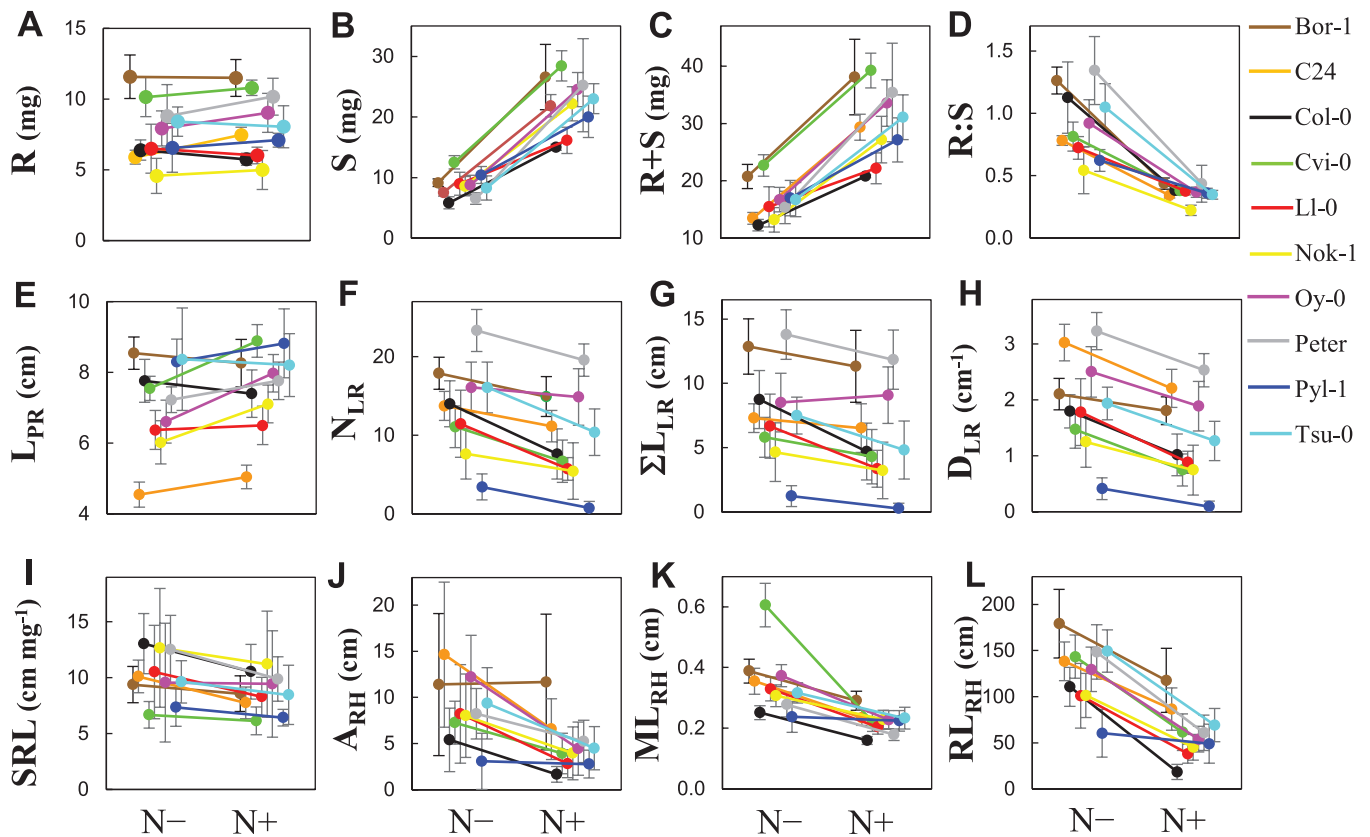
Fig. 2. Biomass production, root morphology, and root hair traits of Arabidopsis accessions in response to nitrate supply. Plants were cultivated with 0.01 mM (N−) or 10 mM nitrate (N+) supplies, as described in Fig. 1. Biomass production (A–D), root morphology (E–I), and root hair (J–L) traits. (A) Root fresh biomass (R); (B) shoot fresh biomass (S); (C) total fresh biomass (R+S); (D) root to shoot biomass ratio (R:S); n=4 × 5 pooled organs ±SD; (E) length of the primary root (L_{PR}); (F) number of lateral roots longer than 1 mm length (N_{LR}); (G) sum of the length of lateral roots (ΣL_{LR}); (H) lateral root density (D_{LR}); (I) specific root length (SRL); (J) area of root hair (A_{RH}); (K) mean root hair length (ML_{RH}), and (L) root hair-forming root length (RL_{RH}); n=15–20 root organs ±SD. Fixed effects models are shown in Supplementary Table S2.

could be identified (Fig. 5B). The N− treatment had a weak influence on R biomass, but a severe decrease of S biomass production, stimulation of lateral root outgrowth, and proliferation of root hairs. The majority of accessions followed the same trajectory in response to N supply (Fig. 5B), with the exception of Col-0 and Ll-0. These two accessions stood apart because they responded the most to N− by increasing R biomass, N_{LR}, ΣL_{LR}, and RL_{RH}. Therefore, the N supply response of the reference accession Col-0 is probably not representative of the whole Arabidopsis species.

To support the results of the PCA, a regression model was adapted to evaluate which traits drove total biomass production (Supplementary Table S4). Combining both N treatments, the largest drivers were L_{PR} (7.8% of total experimental variance), ΣL_{LR} (0.3%), and A_{RH} (0.2%). If accounting for N treatment, either as an interaction or in analyzing N treatment separately, ML_{RH} explained ~99% of experimental variance for R+S biomass in both N+ and N− conditions (Supplementary Table S4), probably related to reduced variation between Petri dishes (Supplementary Fig. S1) that came from taking the mean of root hair length.

Natural variability of nitrate uptake and expression levels of nitrate transporters

The stable isotope ^{15}N was used to determine the short-term root nitrate influx and the allocation between root and shoot organs. In the third experiment, high (HATS) or low (LATS) nitrate affinity transport system activities were measured with seedlings grown on N− or N+ media (Fig. 6A). The LATS values in seedlings cultivated at N+ were more dispersed than the HATS values in those at N−. The Tsu-0 and Pyl-1 accessions showed the lowest HATS and LATS values, while Petergof and Col-0 showed the greatest ones (Fig. 6A). The short-term translocation of ^{15}N between organs (^{15}N $Q_{R:S}$) was calculated as the ^{15}N ratio of the root to the shoot (Fig. 6B). Accessions translocated proportionally less ^{15}N tracer toward aerial parts in N− than in N+ conditions. The Bor-1 and C24 accessions had the least and the greatest ^{15}N $Q_{R:S}$ in N−, respectively, while C24 and Pyl-1 had those in N+.

In the fourth experiment, the expression of genes encoding nitrate transporters was monitored in whole root and shoot tissues (Fig. 6C–J). Levels of *NRT2.1* transcripts in roots were
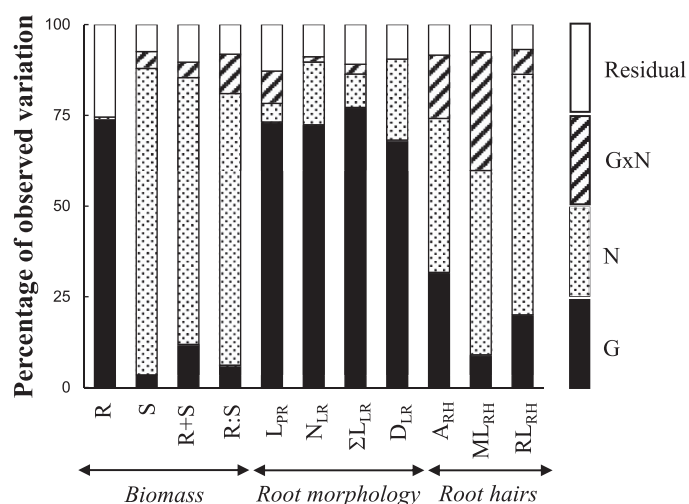
Fig. 3. Variance components analysis for biomass production, root morphology, and root hair traits in Arabidopsis accessions. Histograms show the effects due to accession (G), nitrate treatment (N), accession by nitrate treatment interaction (G×N), and residual unexplained experimental error, as a percentage of the variation explained. Variance components are shown in Supplementary Table S3.

greater than those of any other measured transporter. Levels of *NRT1.7/NPF2.13*, *NRT1.8/NPF7.2*, and *NRT2.2* transcripts were greater in N− than in N+ conditions for all accessions. Globally, *NRT1.2/NPF4.6* and *NRT1.5/NPF7.3* were more highly expressed at N− than at N+, while *NRT1.7/NPF2.13*, *NRT1.8/NPF7.2*, and *NRT1.1/NPF6.3* tended to show the opposite pattern. The Pyl-1 accession was characterized by the lowest *NRT1.2*, *1.4*, *1.5*, and *1.8* expression levels at N− and of the greatest at N+, and among the highest *NRT2.1* and *NRT2.2* expression levels at N−. Petergof had the lowest *NRT2.1* and *2.2* levels at N−.

Investigation of relationships between all measured traits

Pearson correlation coefficients were calculated between measured traits across all four experiments (Fig. 7). Significant correlations described here were noted at ($P<0.01$). At N+, the R and S biomass measures correlated positively ($r=0.90$). The root hair traits positively correlated with various biomass production and root morphological traits ($0.67<r<0.80$) during N− or N+ conditions. In N+, the strongest correlation with R+S biomass was with RL_{RH}, while in N− the strongest correlation was with ML_{RH}, though all three root hair variables were strongly correlated with each other. At N−, ΣL_{LR} correlated positively with the HATS-mediated nitrate uptake rate ($r=0.71$). Also at N−, the R biomass and D_{LR} correlated negatively with *NRT1.1/NPF6.3* ($r=-0.83$) and *NRT2.2* ($r=-0.71$) expression levels, respectively. At N+, L_{PR} correlated negatively with *NRT2.2* expression levels ($r=-0.78$). Also at N+, N_{LR}, ΣL_{LR}, and D_{LR} negatively correlated with *NRT1.5/*

NPF7.3 expression levels ($-0.81<r<-0.75$). Because of that correlation, we further investigated the role of NRT1.5/NPF7.3 in root morphology in relation to nitrate availability. In the fifth experiment, two *nrt1.5/npf7.3* mutant lines in the Col-0 background were grown with 0.1, 1, or 10 mM nitrate. The mutants showed no noticeable root morphology difference compared with the wild type at 0.1 mM or 1 mM nitrate, but they had longer lateral roots at 10 mM nitrate (Supplementary Fig. S3; Supplementary Table S5). Therefore, *NRT1.5/NPF7.3* loss of function rendered lateral root outgrowth less susceptible to the suppression exerted by elevated nitrate supply.

Finally, a hierarchical clustering analysis of the accessions was performed with all phenotypic traits (Fig. 8). The dissimilarity cut-off defined two distinct groups and three single accessions. A first group containing the three accessions Ll-0, Nok-1, and Pyl-1 produced low biomass and was characterized by poor lateral root development, few root hairs, low nitrate uptake rates, and high expression levels of *NRT2.1* or of *NRT2.2* at N− and of *NRT1.5/NPF7.3* at N+. A second group containing the four accessions C24, Cvi-0, Oy-0, and Tsu-0 produced fair biomass (except Cvi-0) and showed intermediate root system sizes. Three other accessions were set apart: (i) Bor-1 had the largest root system size and root hair-forming root length, together with important nitrate uptake rates; (ii) Col-0 produced the lowest biomass but showed large phenotypic plasticity to N treatment; and (iii) Petergof produced much lower shoot biomass at N− compared with N+, and showed the second largest root system size, the greatest HATS-mediated nitrate uptake rate, and low *NRT2.1* and *2.2* expression levels at N−. Remarkably, Bor-1 and Cvi-0 exhibited the greatest total biomasses across the two N treatments. Bor-1 achieved great biomass production through an increased root system size, while Cvi-0 achieved this through profuse root hair development. Taken together, these results highlight the diversity of adaptive responses to N availability and illustrate the importance of monitoring multiple root functional and morphological traits for N acquisition and plant productivity.

Discussion

Root system architecture is of prime importance for exploring soil and capturing resources. This study illustrated the degree of natural variation for root traits of Arabidopsis accessions in response to environmental nitrate supply and how that variability impacted the plant growth and the capacity for nitrate acquisition.

Premises on ideal root architectural attributes to optimize biomass production

The root organ of Arabidopsis has been thoroughly studied and may serve as a resource base for crop breeders. The Arabidopsis model species (De Pessemier *et al.*, 2013) and the closely
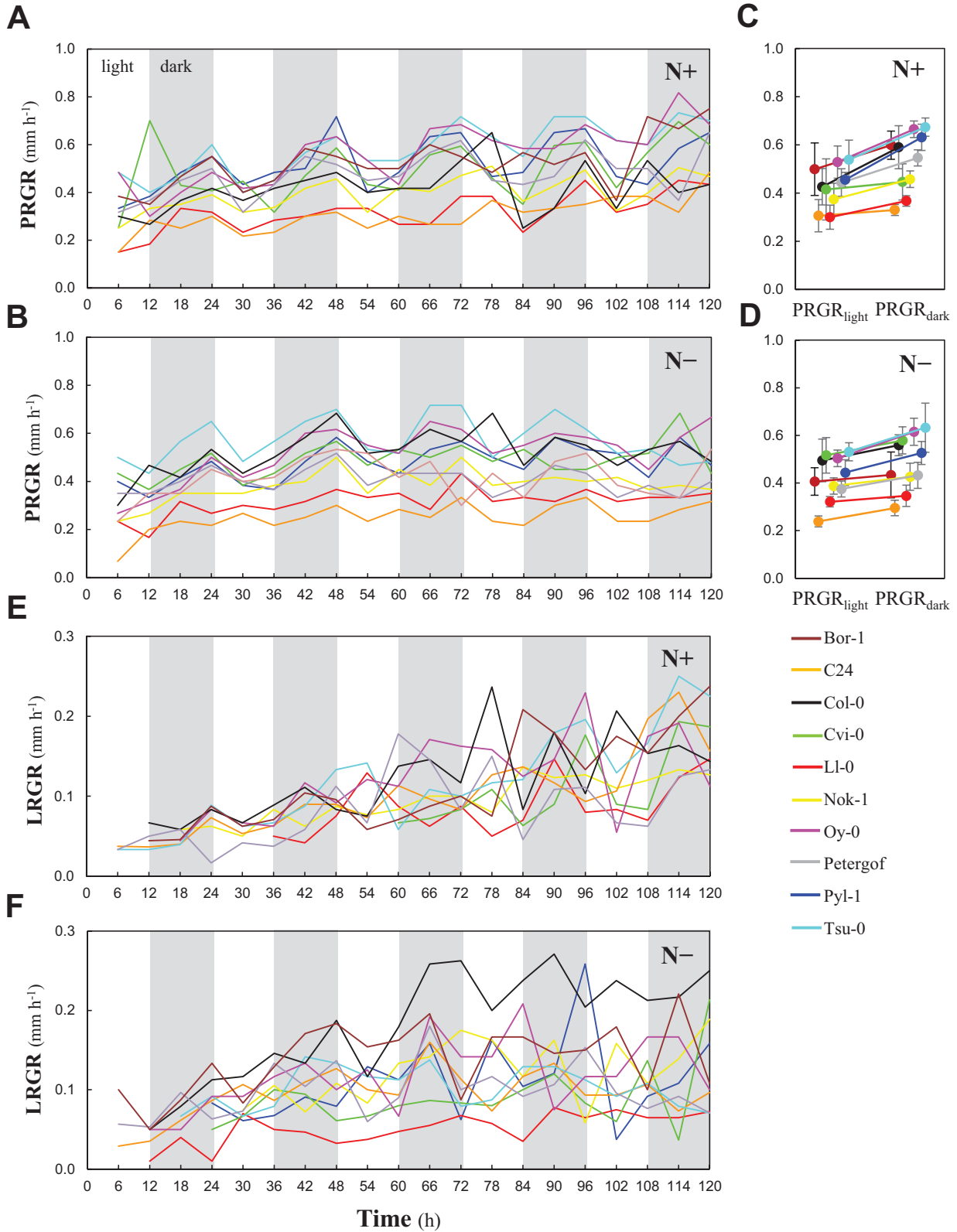
Fig. 4. Root growth kinetics of Arabidopsis accessions in response to nitrate supply. Measurements were taken 6 d after germination every 6 h for 120 h. (A, B) Primary root growth rate (PRGR). (C, D) Average primary root growth rate calculated during the light (PRGR$_{light}$) or the dark period (PRGR$_{dark}$) over four monitoring cycles. (E, F) First emerged lateral root growth rate (LRGR); accessions were grown with 0.01 mM (N−) (A, C, E) or 10 mM (N+) (B, D, F) nitrate supplies. *n*=10 seedlings. Error bars represent SD.

A

B
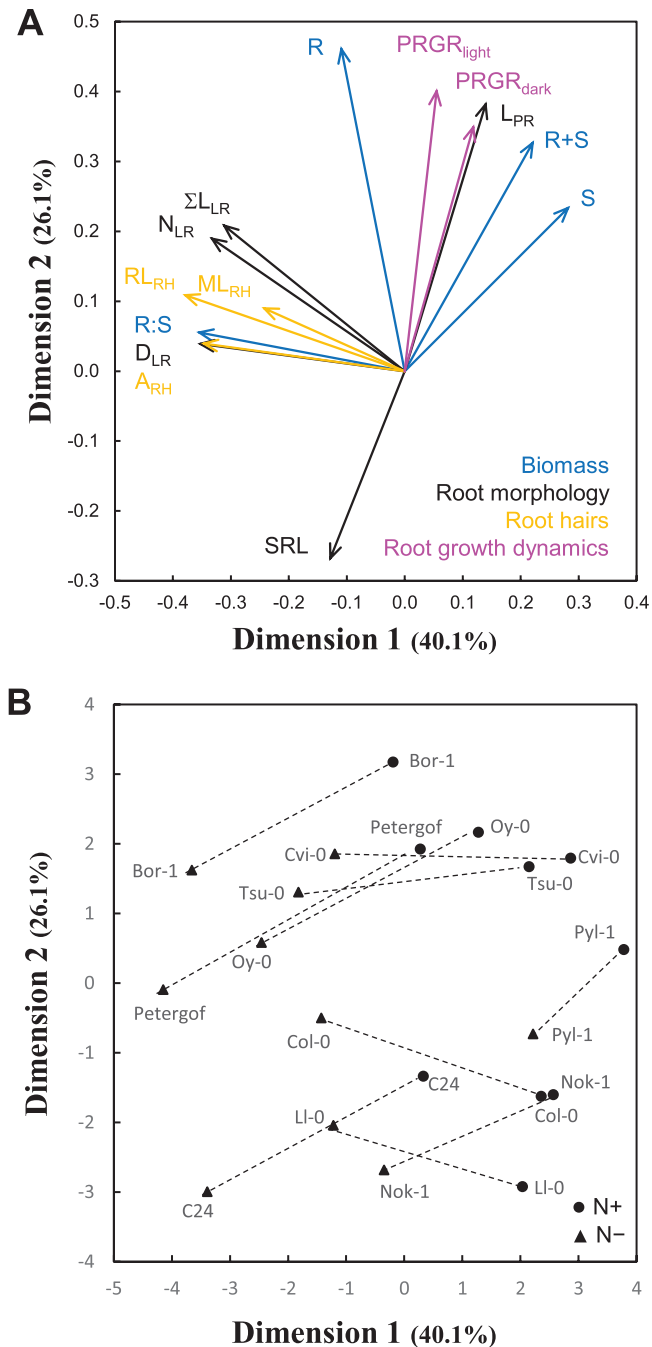
Fig. 5. Principal component analysis of biomass production, root morphology, and root hair traits in Arabidopsis accessions. Variables were measured at 0.01 mM (N–) or 10 mM (N+) nitrate supplies, as described in Fig. 1. Definitions are given in Table 1. (A) Representation of the variables. Correlations between 12 traits mapped onto the first two principal components PC1 and PC2, with cumulative variance of 40.1% and 26.1%, respectively. (B) Representation of the accessions. Symbols indicate the position of the accessions as determined by their trait values in the two principal components. Triangles refer to N– and circles to N+ conditions.

related *Brassica napus* L. (oilseed rape) crop (Kupcsik *et al.*, 2021) show similar root morphological and biomass allocation response to nitrate supply. For instance, low nitrate promotes

lateral root growth while it represses shoot biomass, resulting in greater root to shoot biomass ratio. The natural diversity of Arabidopsis root phenotypes (Fig. 1) provides a framework to identify root characteristics of great value for biomass production in response to nitrate supply. Some accessions demonstrate common root traits that enhance biomass production under varying nutritional conditions, particularly great root allocation patterns.

The accessions Bor-1, Oy-0, Petergof, and Tsu-0 fit the 'steep, cheap, and deep' root ideotype defined by Lynch (2013, 2019). Attributes of that ideotype limiting nitrate leaching in soil are a wide root surface area and long lateral roots with a steep angle. These accessions were among those with the greatest total biomass under both N conditions. Yet, Cvi-0 had a lower specific root length but it still managed to produce a similar biomass to the others. Therefore, the cost of larger root systems does not necessarily impact shoot biomass production, as root and shoot biomass were positively correlated at N+ (Fig. 7B).

Breeding crops that have an optimal root growth in time and space could improve productivity. Indeed, a timely response of root growth may be a major factor determining the capacity to forage soil resources (Lynch, 2013). The rhythmicity of the primary and lateral root growth was compared between the Arabidopsis accessions under light/dark cycles (Fig. 4). Although the primary root length increase was almost constant from day to day, the root growth rate varied during the day. For most accessions, the primary root growth rate showed a maximum at the end of the night, followed by a progressive decrease during the light phase with a minimum at the end of the day, and a gradual recovery throughout the dark phase. This was already reported in early studies with the Col-0 accession cultivated under light/dark and continuous light regimes (Yazdanbakhsh and Fisahn, 2010; Yazdanbakhsh *et al.*, 2011). The importance of starch turnover was emphasized for avoiding transient periods of carbon starvation to sustain root growth during the night. The growth rates varied greatly between accessions (Fig. 4). The Tsu-0 accession had the fastest primary root growth rate during both N treatments and the fastest lateral root growth rate during N+. Tus-0 was previously identified as a high NUE genotype during sand or hydroponic culture at a later developmental stage (Chardon *et al.*, 2010; Masclaux-Daubresse and Chardon, 2011; Menz *et al.*, 2018). Hence, our observations in seedlings advocate for root growth optimization as a valuable screening strategy to improve NUE.

Beneficial root hair traits to enhance plant productivity

Root hairs increase the surface area of roots for nutrient acquisition with a modest biomass investment. The Arabidopsis accessions exhibited substantial variation in root hair characteristics (Supplementary Fig. S2). Low nitrate supply stimulated the proliferation of root hairs (Fig. 2J–L). While the RL_{RH} correlated positively with total biomass in N+ conditions, ML_{RH}
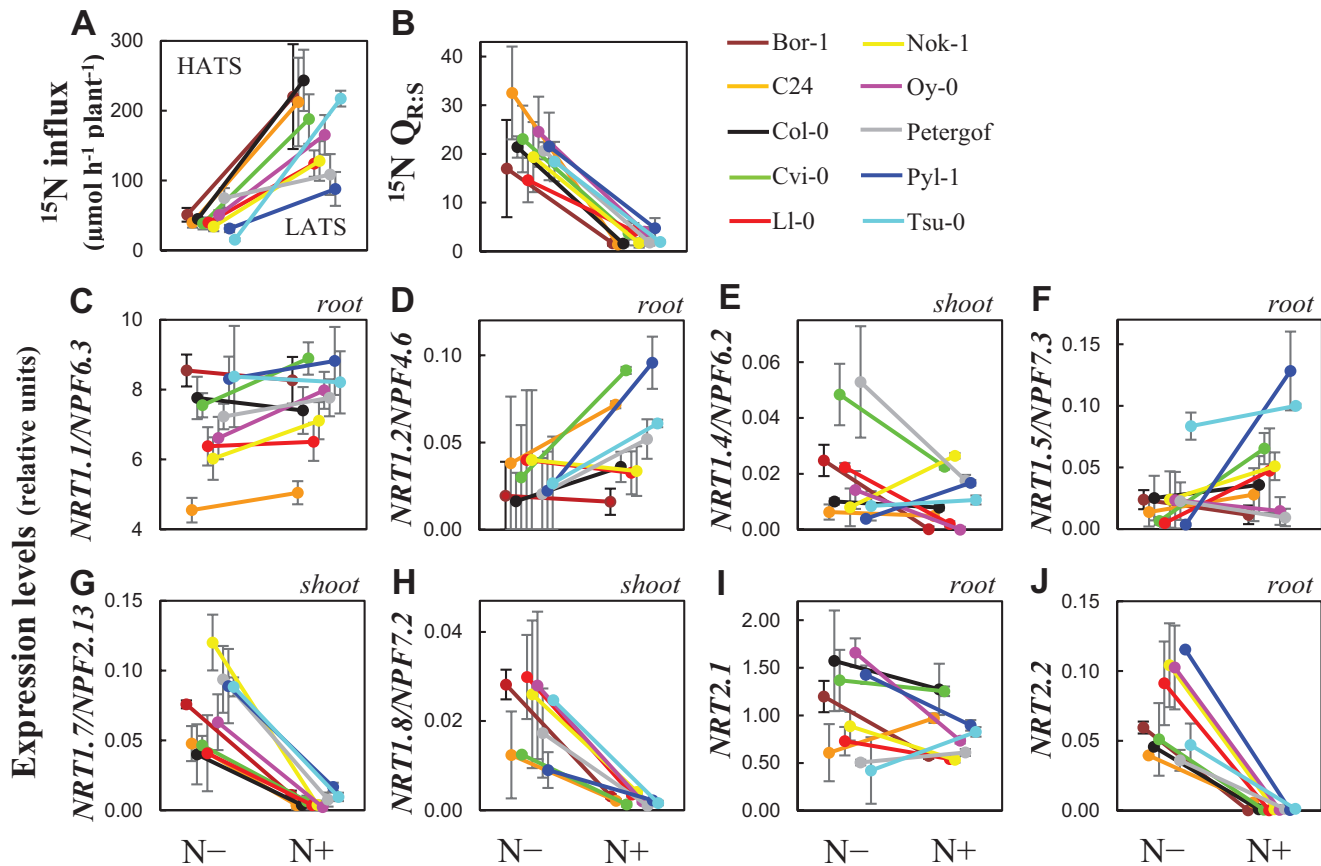
Fig. 6. Nitrate uptake capacities and expression levels of genes involved in nitrate transport of Arabidopsis accessions. Plants were cultivated with 0.01 mM (N–) or 10 mM nitrate (N+) supplies, as described in Fig. 1. (A) Root ^{15}N influx mediated by HATS (HATS ^{15}N influx) or by LATS (LATS ^{15}N influx). (B) Root to shoot ^{15}N quantity (^{15}N $Q_{R:S}$); *n*=6–8 replicates ±SD. Expression levels of (C) *NITRATE TRANSPORTER 1.1* (*NRT1.1*), (D) *NRT1.2*, (E) *NRT1.4*, (F) *NRT1.5*, (H) *RNT1.7*, (G) *NRT1.8*, (H) *NRT2.1*, and (I) *NRT2.2*. Expression levels of *NRT1.1*, *NRT1.2*, *NRT2.1*, and *NRT2.2* were measured in roots and those of *NRT1.4*, *NRT1.5*, *NRT1.7*, and *NRT1.8* in shoots. The expression levels were determined by RT–qPCR on mRNA pools from 20 seedlings and normalized with *ACTIN2* and *UBIQITIN10* signals. Data are means of two biological replicates ±SE (each sample assessed by three technical replicates).

did with total biomass in N− (Fig. 7). These root hair pheno-typic observations support earlier modeling describing diffusion rates. Nye (1966) and Itoh and Barber (1983) suggested that when root hairs are co-located at high densities, the length of the root hairs is the most important factor. The diffusion into the root hairs would create a very low concentration of solutes near the base of the hairs, while diffusion would remain great at the tip. Thus, long root hairs would provide a soil exploration function. Under N−, the exploratory function of root hair phenotypes is observed (Supplementary Fig. S2). Under N+, the root length on which root hairs are formed may provide a low-resistance pathway, while long root hairs are not beneficial because of abundant nitrate near the root surface. Furthermore, Saengwilai *et al.* (2021) found that long root hairs enhanced growth in *Zea mays* L. (maize) and responded to nitrate concentrations. In the present study, the whole root system phenotype differed depending on N supply, with A_{RH} and ML_{RH} showing the strongest G×N interaction (Supplementary Table S3). This genotype by environment phenotypic variation may

explain contrasting root hair results in previous studies, such as those noted by Keyes *et al.* (2013). The important G×N interaction suggests the possibility of selecting genotypes with many root hairs that only grow long under low N supply. The same genotype would save investment in additional root hair growth for conditions under which it would enhance nutrient uptake. For instance, Cvi-0 had a similar ML_{RH} to other accessions under N+ but grew very long root hairs under N- (Fig. 2; Supplementary Fig. S2).

One potentially contrasting observation to the above argument is the positive correlation of the RL_{RH} with the root biomass in both N conditions (Fig. 7). Increased root growth may increase the total opportunity for root hair formation. Additionally, the strong correlation among all root hair variables suggests a possible confounding of the three root hair variables. The random effects model (Supplementary Table S4) suggested that ML_{RH} was the strongest predictor of total biomass under both N conditions. This is likely to be largely due to the precision of the estimates, in which the coefficients of
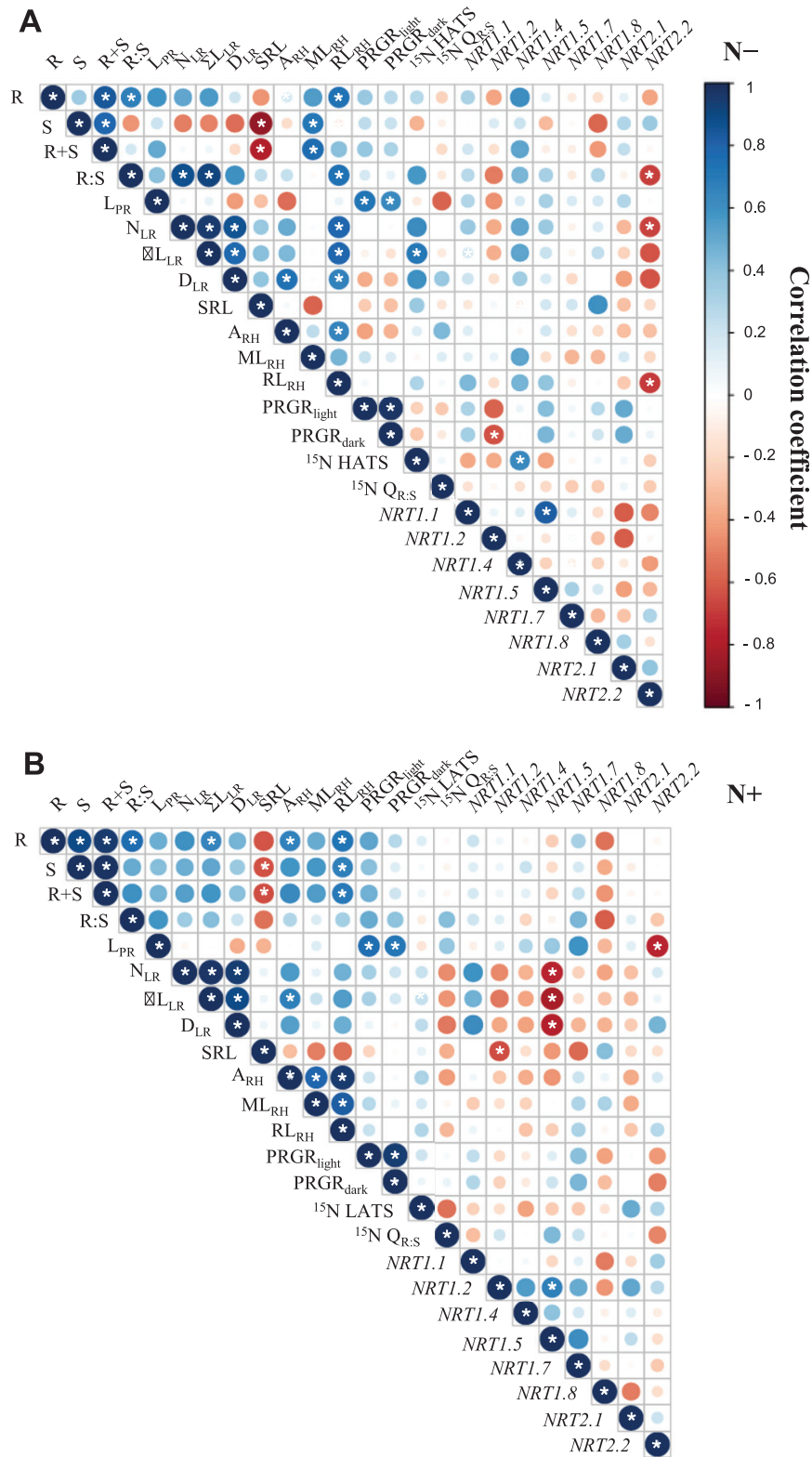
Fig. 7. Correlations between all measured traits in Arabidopsis accessions. The following traits were measured during experiments 1–4, in seedlings grown with 0.01 mM (N–) (A) or 10 mM (N+) (B) nitrate supplies. Traits are defined in Table 1. The size of the circle area is proportional to the absolute value of the correlation coefficient. Blue or red colors indicate positive or negative correlations. Asterisks indicate a correlation coefficient significantly (P<0.01) different from zero.
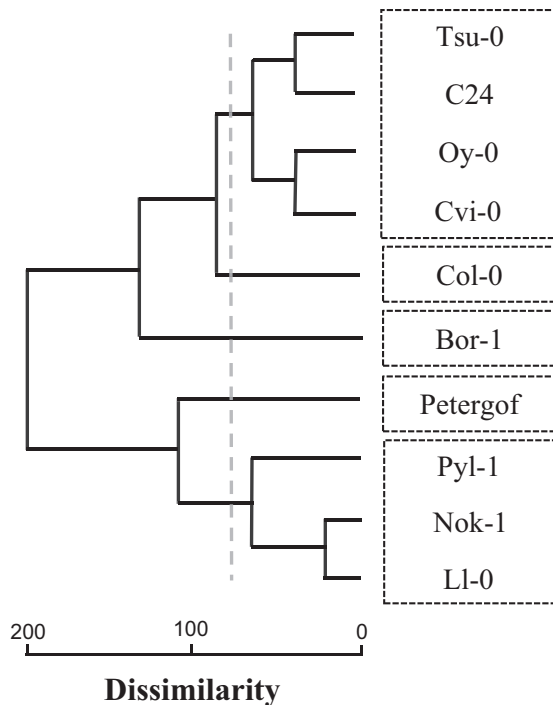
Fig. 8. Ascendant hierarchical classification of Arabidopsis accessions. The dendrogram was performed by computing data of the biomass production, root morphology, root hairs, nitrate uptake influxes, and expression levels of genes involved in nitrate transport obtained from seedling plants grown with 0.01 mM (N−) or 10 mM (N+). Two groups and three individual accessions were identified.

variation for both RL_{RH} and A_{RH} are greater than those for ML_{RH} (Fig. 2J–L). As a methodological outcome of more observations (Lane and Murray, 2021), the ML_{RH} averages multiple measurements per plant, while RL_{RH} and A_{RH} are single measurements per plant, and thus exhibit a more variable phenotype. An interpretation of the high correlation between total biomass and RL_{RH} under N+ (Fig. 7B) is that RL_{RH} may enhance growth only under nitrate-sufficient conditions. That explanation is consistent with long-standing models of solute fluxes in root hair complexes mentioned above. In any case, root hair characteristics were both highly plastic and strong predictors of growth under both N conditions.

Multiple factors influencing nitrate acquisition

The promotion of lateral root development together with increased expression and activity of nitrate transporters are major adaptive responses of the root system to low nitrate conditions (Zhang and Forde, 2000; Remans *et al.*, 2006b; Kiba and Krapp, 2016). The lateral root length and HATS-mediated nitrate influx positively correlated at N− (Fig. 7A). The accessions Bor-1, Oy-0, and Petergof exhibited numerous and long lateral roots (Fig. 2F, G) together with important HATS-mediated nitrate influx (Fig. 6A). In contrast, Nok-1 and Pyl-1 produced very few lateral roots and presented little influx. Therefore,

accessions with a broader root surface took up more nitrate under these conditions. However, the absence of such a correlation at N+ (Fig. 7B) indicated that the number and/or the activity of nitrate transporters are also of primary importance for determining the overall nitrate uptake rate. In a similar study conducted with a diversity panel comprising modern oilseed rape cultivars (Kupcsik *et al.*, 2021), the nitrate influxes correlated positively with the total root length.

There were also correlations among root biomass, morphological traits, and the expression levels of some nitrate transporter-encoding genes. The expression study (Fig. 6C–J) was conducted on whole root tissues at different stages of lateral root formation. Therefore, it provided only average gene expression levels on all types of root cells, while N responses are, to a large extent, cell type specific (Kortz and Hochholdinger, 2019). During both N conditions, *NRT1.2/NPF4.6* and *NRT2.2* transcript levels negatively correlated with some root traits (Fig. 7). With N+ supply, *NRT1.5/NPF7.3* transcript levels negatively correlated with the sum of the lengths of lateral roots (Fig. 7B). NRT1.5/NPF7.3 is depicted as a low-affinity nitrate transporter that drives xylem loading from the root pericycle and root to shoot translocation (Lin *et al.*, 2008) and as a proton/potassium antiporter (Drechsler *et al.*, 2015; Li *et al.*, 2017a). Furthermore, NRT1.5/NPF7.3 mediates transport of indole-3-butyric acid (IBA), a precursor of the endogenous auxin indole-3-acetic acid (IAA) which is involved in root gravitropic responses (Watanabe *et al.*, 2020). Loss of function causes reduced lateral root density during potassium (Zheng *et al.*, 2016) and phosphorus (Cui *et al.*, 2019) deficiencies. At high nitrate supply, two *nrt1.5/npf7.3* mutants exhibited increased lateral root length compared with wild-type plants (Supplementary Fig. S3). This suggests that NRT1.5/NPF7.3 may act as a repressor of lateral root growth during nitrate repletion. It then mirrors the role of NRT1.1/NPF6.3 that represses lateral root development when nitrate is scarce (Remans *et al.*, 2006a; Mounier *et al.*, 2014; Bouguyon *et al.*, 2016). Taken together, these data illustrate the major role of *NRT1/NPF* genes in the control of root development in response to nitrate availability. Finally, an ideotype that would have very low levels of *NRT1.1/NPF6.3* in lateral root primordia during low nitrate availability, and low expression of *NRT1.5/NPF7.3* during elevated nitrate, would maintain lateral root outgrowth to optimize soil foraging under both scenarios.

Conclusion

This study uncovered substantial root phenotypic variation and adaptative responses to N availability. It also illustrated the complexity of factors shaping root morphology and regulating N uptake. Notably, a large root system can produce great above-ground biomass. This work clarified one performant ideotype that would rapidly develop a highly branched and deep root system, with greater root hair development and with

greater N uptake capacity. Arabidopsis is a good model to identify possible target root phenes to increase plant productivity.

Supplementary data

The following supplementary data are available at *JXB* online.

Fig. S1. Illustration of Arabidopsis seedlings grown *in vitro* in Petri dishes.

Fig. S2. Representative root hair phenotypes of two Arabidopsis accessions in response to nitrate supply.

Fig. S3. T-DNA insertion sites in the mutant lines *nrt1.5/npf7.3* and root morphology in response to nitrate supply.

Table S1. Primer sequences for qPCR.

Table S2. Fixed effects models from experiment 1.

Table S3. Variance components estimates of the accessions with all random effects for the dataset from experiment 1.

Table S4. Simple linear regression model applied to the dataset from experiment 1.

Table S5. Fixed effects models for the root morphology data set of wild-type and *nrt1.5/npf7.3* mutant lines from experiment 5.

Conflict of interest

The authors have no conflicts to declare.

Data availability

The data supporting the findings of this study are available from the corresponding author, Christian Hermans, upon request.

References

Asim M, Ullah Z, Xu F, An L, Aluko OO, Wang Q, Liu H. 2020. Nitrate signaling, functions, and regulation of root system architecture: insights from *Arabidopsis thaliana*. Gene **11**, 633.

Banda J, Bellande K, von Wangenheim D, Goh T, Guyomarc'h S, Laplaze L, Bennett MJ. 2019. Lateral root formation in Arabidopsis: a well-ordered LRexit. Trends in Plant Science **24**, 826–839.

Bates D, Machler M, Bolker B, Walker S. 2015. Fitting linear mixed-effects models using {lme4}. Journal of Statistical Software **67**, 1–48.

Bouguyon E, Perrine-Walker F, Pervent M, *et al*. 2016. Nitrate controls root development through posttranscriptional regulation of the NRT1.1/NPF6.3 transporter/sensor. Plant Physiology **172**, 1237–1248.

Canales J, Contreras-López O, Álvarez JM, Gutiérrez RA. 2017. Nitrate induction of root hair density is mediated by TGA1/TGA4 and CPC transcription factors in *Arabidopsis thaliana*. The Plant Journal **92**, 305–316.

Chardon F, Barthélémy J, Daniel-Vedele F, Masclaux-Daubresse C. 2010. Natural variation of nitrate uptake and nitrogen use efficiency in *Arabidopsis thaliana* cultivated with limiting and ample nitrogen supply. Journal of Experimental Botany **61**, 2293–2302.

Chen KE, Chen HY, Tseng CS, Tsay YF. 2020. Improving nitrogen use efficiency by manipulating nitrate remobilization in plants. Nature Plants **6**, 1126–1135.

Chiu C-C, Lin C-S, Hsia A-P, Su R-C, Lin H-L, Tsay Y-F. 2004. Mutation of a nitrate transporter, AtNRT1:4, results in a reduced petiole nitrate content and altered leaf development. Plant & Cell Physiology **45**, 1139–1148.

Cui YN, Li XT, Yuan JZ, Wang FZ, Wang SM, Ma Q. 2019. Nitrate transporter NPF7.3/NRT1.5 plays an essential role in regulating phosphate deficiency responses in Arabidopsis. Biochemical and Biophysical Research Communications **508**, 314–319.

De Pessemier J, Chardon F, Juraniec M, Delaplace P, Hermans C. 2013. Natural variation of the root morphological response to nitrate supply in *Arabidopsis thaliana*. Mechanisms of Development **130**, 45–53.

Drechsler N, Zheng Y, Bohner A, Nobmann B, von Wirén N, Kunze R, Rausch C. 2015. Nitrate-dependent control of shoot K homeostasis by the Nitrate Transporter1/Peptide Transporter Family member NPF7.3/NRT1.5 and the Stelar K$^+$ Outward Rectifier SKOR in Arabidopsis. Plant Physiology **169**, 2832–2847.

Fan S-C, Lin C-S, Hsu P-K, Lin S-H, Tsay Y-F. 2009. The *Arabidopsis* nitrate transporter NRT1.7, expressed in phloem, is responsible for source-to-sink remobilization of nitrate. The Plant Cell **21**, 2750–2761.

Fan X, Tang Z, Tan Y, Zhang Y, Luo B, Yang M, Lian X, Shen Q, Miller AJ, Xu G. 2016. Overexpression of a pH-sensitive nitrate transporter in rice increases crop yields. Proceedings of the National Academy of Sciences, USA **113**, 7118–7123.

Fanzo J, Covic N, Dobermann A, Henson S, Herrero M, Pingali P, Staal S. 2020. A research vision for food systems in the 2020s: defying the status quo. Global Food Security **26**, 100397.

Gifford ML, Banta JA, Katari MS, Hulsmans J, Chen L, Ristova D, Tranchina D, Purugganan MD, Coruzzi GM, Birnbaum KD. 2013. Plasticity regulators modulate specific root traits in discrete nitrogen environments. PLoS Genetics **9**, e1003760.

Hermans C, Porco S, Verbruggen N, Bush DR. 2010. Chitinase-like protein CTL1 plays a role in altering root system architecture in response to multiple environmental conditions. Plant Physiology **152**, 904–917.

Hu B, Wang W, Ou S, *et al*. 2015. Variation in NRT1.1B contributes to nitrate-use divergence between rice subspecies. Nature Genetics **47**, 834–838.

Huang NC, Liu KH, Lo HJ, Tsay YF. 1999. Cloning and functional characterization of an Arabidopsis nitrate transporter gene that encodes a constitutive component of low-affinity uptake. The Plant Cell **11**, 1381–1392.

Itoh S, Barber SA. 1983. A numerical solution of whole plant nutrient uptake for soil–root systems with root hairs. Plant and Soil **70**, 403–413.

Jia Z, Giehl RFH, Meyer RC, Altmann T, von Wirén N. 2019. Natural variation of BSK3 tunes brassinosteroid signaling to regulate root foraging under low nitrogen. Nature Communications **10**, 2378.

Jia Z, Giehl RFH, von Wirén N. 2020. The root foraging response under low nitrogen depends on *DWARF1*-mediated brassinosteroid biosynthesis. Plant Physiology **183**: 998–1010.

Jia Z, Giehl RFH, von Wirén N. 2021. Local auxin biosynthesis acts downstream of brassinosteroids to trigger root foraging for nitrogen. Nature Communications **12**, 5437.

Jia Z, von Wirén N. 2020. Signaling pathways underlying nitrogen-dependent changes in root system architecture: from model to crop species. Journal of Experimental Botany **71**, 4393–4404.

Jungk A. 2001. Root hairs and the acquisition of plant nutrients from soil. Journal of Plant Nutrition and Soil Science **164**, 121–129.

Keyes SD, Daly KR, Gostling NJ, Jones DL, Talboys P, Pinzer BR, Boardman R, Sinclair I, Marchant A, Roose T. 2013. High resolution synchrotron imaging of wheat root hairs growing in soil and image based modelling of phosphate uptake. New Phytologist **198**, 1023–1029.

Kiba T, Feria-Bourrellier A-B, Lafouge F, *et al*. 2012. The Arabidopsis nitrate transporter NRT2.4 plays a double role in roots and shoots of nitrogen-starved plants. The Plant Cell **24**, 245–258.

Kiba T, Krapp A. 2016. Plant nitrogen acquisition under low availability: regulation of uptake and root architecture. Plant & Cell Physiology **57**, 707–714.

Kortz A, Hochholdinger F, Yu P. 2019. Cell type-specific transcriptomics of lateral root formation and plasticity. Frontiers in Plant Science **10**, 21.

Krouk G, Lacombe B, Bielach A, *et al*. 2010. Nitrate-regulated auxin transport by NRT1.1 defines a mechanism for nutrient sensing in plants. Developmental Cell **18**, 927–937.

Krouk G, Tillard P, Gojon A. 2006. Regulation of the high-affinity NO_3^- uptake system by NRT1.1-mediated NO_3^- demand signaling in Arabidopsis. Plant Physiology **142**, 1075–1086.

Kupcsik L, Chiodi C, Moturu TR, *et al.* 2021. Oilseed rape cultivars show diversity of root morphologies with the potential for better capture of nitrogen. Nitrogen **2**, 491–505.

Lane HM, Murray SC. 2021. High throughput can produce better decisions than high accuracy when phenotyping plant populations. Crop Science **61**, 3301–3313.

Laugier E, Bouguyon E, Mauriès A, Tillard P, Gojon A, Lejay L. 2012. Regulation of high-affinity nitrate uptake in roots of Arabidopsis depends predominantly on posttranscriptional control of the NRT2.1/NAR2.1 transport system. Plant Physiology **158**, 1067–1078.

Léran S, Varala K, Boyer J-C, *et al*. 2014. A unified nomenclature of NITRATE TRANSPORTER 1/PEPTIDE TRANSPORTER family members in plants. Trends in Plant Science **19**, 5–9.

Lezhneva L, Kiba T, Feria-Bourrellier AB, Lafouge F, Boutet-Mercey S, Zoufan P, Sakakibara H, Daniel-Vedele F, Krapp A. 2014. The Arabidopsis nitrate transporter NRT2.5 plays a role in nitrate acquisition and remobilization in nitrogen-starved plants. The Plant Journal **80**, 230–241.

Li H, Hu B, Chu C. 2017b. Nitrogen use efficiency in crops: lessons from Arabidopsis and rice. Journal of Experimental Botany **68**, 2477–2488.

Li H, Yu M, Du XQ, Wang ZF, Wu WH, Quintero FJ, Jin XH, Li HD, Wang Y. 2017a. NRT1.5/NPF7.3 functions as a proton-coupled H^+/K^+ antiporter for K^+ loading into the xylem in Arabidopsis. The Plant Cell **29**, 2016–2026.

Li J-Y, Fu Y-L, Pike SM, *et al*. 2010. The *Arabidopsis* nitrate transporter NRT1.8 functions in nitrate removal from the xylem sap and mediates cadmium tolerance. The Plant Cell **22**, 1633–1646.

Li X, Zeng R, Liao H. 2016. Improving crop nutrient efficiency through root architecture modifications. Journal of Integrative Plant Biology **58**, 193–202.

Lin S-H, Kuo H-F, Canivenc G, *et al*. 2008. Mutation of the *Arabidopsis NRT1.5* nitrate transporter causes defective root-to-shoot nitrate transport. The Plant Cell **20**, 2514–2528.

Louvieaux J, Leclercq A, Haelterman L, Hermans C. 2020a. In-field observation of root growth and nitrogen uptake efficiency of winter oilseed rape. Agronomy **10**, 105.

Louvieaux J, Spanoghe M, Hermans C. 2020b. Root morphological traits of seedlings are predictors of seed yield and quality in winter oilseed rape hybrid cultivars. Frontiers in Plant Science **11**, 568009.

Lynch JP. 2013. Steep, cheap and deep: an ideotype to optimize water and N acquisition by maize root systems. Annals of Botany **112**, 347–357.

Lynch JP. 2019. Root phenotypes for improved nutrient capture: an underexploited opportunity for global agriculture. New Phytologist **223**, 548–564.

Lynch JP, Brown KM. 2012. New roots for agriculture: exploiting the root phenome. Philosophical Transactions of the Royal Society B: Biological Sciences **367**, 1598–1604.

Maghiaoui A, Bouguyon E, Cuesta C, Perrine-Walker F, Alcon C, Krouk G, Benková E, Nacry P, Gojon A, Bach L. 2020. The Arabidopsis NRT1.1 transceptor coordinately controls auxin biosynthesis and transport to regulate root branching in response to nitrate. Journal of Experimental Botany **71**, 4480–4494.

Masclaux-Daubresse C, Chardon F. 2011. Exploring nitrogen remobilization for seed filling using natural variation in *Arabidopsis thaliana*. Journal of Experimental Botany **62**, 2131–2142.

Martínez-Dalmau J, Berbel J, Ordóñez-Fernández R. 2021. Nitrogen fertilization. A review of the risks associated with the inefficiency of its use and policy responses. Sustainability **13**, 5625.

Meng S, Peng JS, He YN, Zhang GB, Yi HY, Fu YL, Gong JM. 2016. Arabidopsis NRT1.5 mediates the suppression of nitrate starvation-induced leaf senescence by modulating foliar potassium level. Molecular Plant **9**, 461–470.

Menz J, Range T, Trini J, Ludewig U, Neuhäuser B. 2018. Molecular basis of differential nitrogen use efficiencies and nitrogen source preferences in contrasting Arabidopsis accessions. Scientific Reports **8**, 3373.

Moll RH, Kamprath EJ, Jackson WA. 1982. Analysis and interpretation of factors which contribute to efficiency of nitrogen utilization. Agronomy Journal **74**, 562–564.

Mounier E, Pervent M, Ljung K, Gojon A, Nacry P. 2014. Auxin-mediated nitrate signalling by NRT1.1 participates in the adaptive response of *Arabidopsis* root architecture to the spatial heterogeneity of nitrate availability. Plant, Cell & Environment **37**, 162–174.

Muratore C, Espen L, Prinsi B. 2021. Nitrogen uptake in plants: the plasma membrane root transport systems from a physiological and proteomic perspective. Plants **10**, 681.

North KA, Ehlting B, Koprivova A, Rennenberg H, Kopriva S. 2009. Natural variation in Arabidopsis adaptation to growth at low nitrogen conditions. Plant Physiology and Biochemistry **47**, 912–918.

Nye PH. 1966. The effect of the nutrient intensity and buffering power of a soil, and the absorbing power, size and root hairs of a root, on nutrient absorption by diffusion. Plant and Soil **25**, 81–105.

Orsel M, Krapp A, Daniel-Vedele F. 2002. Analysis of the NRT2 nitrate transporter family in Arabidopsis. Structure and gene expression. Plant Physiology **129**, 886–896.

Ota R, Ohkuko Y, Yamashita Y, Ogawa-Ohnishi M, Matsubayashi Y. 2020. Shoot-to-root mobile CEPD-like 2 integrates shoot nitrogen status to systemically regulate nitrate uptake in Arabidopsis. Nature Communications **11**, 641.

Pierret A, Maeght J-L, Clément C, Montoroi J-P, Hartmann C, Gonkhamdee S. 2016. Understanding deep roots and their functions in ecosystems: an advocacy for more unconventional research. Annals of Botany **118**, 621–635.

Pound MP, French AP, Atkinson JA, Wells DM, Bennett MJ, Pridmore T. 2013. RootNav: navigating images of complex root architectures. Plant Physiology **162**, 1802–1814.

Pradhan P, Fischer G, van Velthuizen H, Reusser DE, Kropp JP. 2015. Closing yield gaps: how sustainable can we be? PLoS One **10**, e0129487.

R Core Team. 2019. R: a language and environment for statistical computing. Vienna, Austria: R Foundation for Statistical Computing.

Remans T, Nacry P, Pervent M, Filleur S, Diatloff E, Mounier E, Tillard P, Forde BG, Gojon A. 2006a. The *Arabidopsis* NRT1.1 transporter participates in the signaling pathway triggering root colonization of nitrate-rich patches. Proceedings of the National Academy of Sciences, USA **103**, 19206–19211.

Remans T, Nacry P, Pervent M, Girin T, Tillard P, Lepetit M, Gojon A. 2006b. A central role for the nitrate transporter NRT2.1 in the integrated morphological and physiological responses of the root system to nitrogen limitation in Arabidopsis. Plant Physiology **140**, 909–921.

Rosas U, Cibrian-Jaramillo A, Ristova D, *et al*. 2013. Integration of responses within and across *Arabidopsis* natural accessions uncovers loci controlling root systems architecture. Proceedings of the National Academy of Sciences, USA **110**, 15133–15138.

Saengwilai P, Strock C, Rangarajan H, Chimungu J, Salungyu J, Lynch JP. 2021. Root hair phenotypes influence nitrogen acquisition in maize. Annals of Botany **128**, 849–858.

Spiertz JHJ. 2010. Nitrogen, sustainable agriculture and food security. A review. Agronomy for Sustainable Development **30**, 43–55.

Stephenson P, Stacey N, Brüser M, Pullen N, Ilyas M, O'Neil C, Wells R, Østergaard L. 2019. The power of model-to-crop translation illustrated by reducing seed loss from pod shatter in oilseed rape. Plant Reproduction **32**, 331–340.

Sun CH, Yu Q, Hu DG. 2017. Nitrate: a crucial signal during lateral roots development. Frontiers in Plant Science **8**, 485.

Vangheluwe N, Beeckman T. 2021. Lateral root initiation and the analysis of gene function using genome editing with CRISPR in Arabidopsis. Genes **12**, 884.

Vatter T, Neuhäuser B, Stetter M, Ludewig U. 2015. Regulation of length and density of Arabidopsis root hairs by ammonium and nitrate. Journal of Plant Research **128**, 839–848.

Vidal EA, Alvarez JM, Araus V, *et al*. 2020. Nitrate in 2020: thirty years from transport to signaling networks. The Plant Cell **32**, 2094–2119.

Vincent C, Rowland D, Na C, Schaffer B. 2016. A high-throughput method to quantify root hair area in digital images taken in situ. Plant and Soil **412**, 61–80.

Watanabe S, Takahashi N, Kanno Y, *et al*. 2020. The *Arabidopsis* NRT1/PTR FAMILY protein NPF7.3/NRT1.5 is an indole-3-butyric acid transporter involved in root gravitropism. Proceedings of the National Academy of Sciences, USA **117**, 31500–31509.

Wells DM, French AP, Naeem A, Ishaq O, Traini R, Hijazi HI, Bennett MJ, Pridmore TP. 2012. Recovering the dynamics of root growth and development using novel image acquisition and analysis methods. Philosophical Transactions of the Royal Society B: Biological Sciences **367**, 1517–1524.

White PJ. 2019. Root traits benefitting crop production in environments with limited water and nutrient availability. Annals of Botany **124**, 883–890.

Yazdanbakhsh N, Fisahn J. 2010. Analysis of *Arabidopsis thaliana* root growth kinetics with high temporal and spatial resolution. Annals of Botany **105**, 783–791.

Yazdanbakhsh N, Sulpice R, Graf A, Stitt M, Fisahn J. 2011. Circadian control of root elongation and C partitioning in *Arabidopsis thaliana*. Plant, Cell & Environment **34**, 877–894.

Zhang H, Forde BG. 2000. Regulation of *Arabidopsis* root development by nitrate availability. Journal of Experimental Botany **51**, 51–59.

Zhang H, Rong H, Pilbeam D. 2007. Signalling mechanisms underlying the morphological responses of the root system to nitrogen in *Arabidopsis thaliana*. Journal of Experimental Botany **58**, 2329–2338.

Zheng Y, Drechsler N, Rausch C, Kunze R. 2016. The Arabidopsis nitrate transporter NPF7.3/NRT1.5 is involved in lateral root development under potassium deprivation. Plant Signaling & Behavior **11**, e1176819.